

POLITECNICO DI TORINO  
Repository ISTITUZIONALE

Multivariate macromodeling with stability and passivity constraints

*Original*

Multivariate macromodeling with stability and passivity constraints / Zanco, Alessandro; Grivet-Talocia, S.; Bradde, Tommaso; DE STEFANO, Marco. - ELETTRONICO. - (2018), pp. 1-4. (Intervento presentato al convegno 22nd IEEE Workshop on Signal and Power Integrity, SPI 2018 tenutosi a Brest, France nel 22-25 May 2018) [10.1109/SaPIW.2018.8401664].

*Availability:*

This version is available at: 11583/2712915 since: 2018-09-13T14:59:54Z

*Publisher:*

Institute of Electrical and Electronics Engineers Inc.

*Published*

DOI:10.1109/SaPIW.2018.8401664

*Terms of use:*

This article is made available under terms and conditions as specified in the corresponding bibliographic description in the repository

*Publisher copyright*

(Article begins on next page)

# Multivariate Macromodeling with Stability and Passivity Constraints

A. Zanco, S. Grivet-Talocia, T. Bradde, M. De Stefano  
 Dept. Electronics and Telecommunications, Politecnico di Torino  
 e-mail stefano.grivet@polito.it

**Abstract**—We present a general framework for the construction of guaranteed stable and passive multivariate macromodels from sampled frequency responses. The obtained macromodels embed in closed form the dependence on external parameters, through a data-driven approximation of input data samples based on orthogonal polynomial bases. The key novel contribution of this work is an extension to the multivariate and possibly high-dimensional case of Hamiltonian-based passivity check and enforcement algorithms, which can be applied to enforce both uniform stability and uniform passivity of the models. The modeling flow is demonstrated on a representative interconnect example.

## I. INTRODUCTION

Passive macromodeling algorithms are now commonly adopted by both academia and industry for fast Signal and Power Integrity simulation of complex interconnects [1]–[3]. Such techniques, now available in practically all Electronic Design Automation (EDA) software suites, are able to construct compact dynamical models of virtually any Linear Time-Invariant (LTI) system or structure, including signal and power distribution networks, discrete components, filters, etc. If passivity is enforced during model construction (thus implying model stability and causality), the models can be reliably used in time-domain simulations for system-level qualification.

The next step towards robust system design would be to perform fully automated simulation-driven optimization. Based on the results of repeated frequency- or time-domain simulations, the system parameters would be changed by a suitable optimizer, until an optimum configuration is found. This approach is already adopted in many cases, but still not fully automated. Manual adjustment of system parameters is routinely performed by SI/PI engineers, who have to repeat costly numerical simulations with significant user interaction. This flow would greatly benefit from the availability of fully parameterized macromodels, which could be used as surrogates for the evaluation of the system responses during the optimization phase with a drastically reduced runtime, thus enabling unsupervised design automation.

Multivariate (parameterized) macromodeling algorithms do exist [4]–[6], with some approaches even being able to enforce passivity by construction [5], [6] through special interpolation rules applied to a grid of possibly scaled and shifted non-parameterized root macromodels. This work provides an alternative approach, based on a more general model structure, for the generation of accurate, robust, uniformly stable and passive multivariate macromodels, by extending to the multivariate

case the well-known Hamiltonian-based passivity check and enforcement algorithms. Due to lack of space, we focus our presentation on the general flow and high-level mathematical aspects, referring the Reader to [1], [4], [7], [8] for a more precise and complete presentation of background material, and to a forthcoming extended publication for full details.

## II. FORMULATION

We consider a  $P$ -port multivariate macromodel in a *Parameterized Sanathanan-Koerner (PSK)* form [4], [9]

$$\mathbf{H}(s; \vartheta) = \frac{\mathbf{N}(s, \vartheta)}{\mathbf{D}(s, \vartheta)} = \frac{\sum_{n=0}^{\bar{n}} \sum_{\ell=1}^{\bar{\ell}} \mathbf{R}_{n,\ell} \xi_{\ell}(\vartheta) \varphi_n(s)}{\sum_{n=0}^{\bar{n}} \sum_{\ell=1}^{\bar{\ell}} r_{n,\ell} \xi_{\ell}(\vartheta) \varphi_n(s)}, \quad (1)$$

where  $s = j\omega$  is the Laplace variable and  $\vartheta \in \Theta \subset \mathbb{R}^{\rho}$  collects additional  $\rho$  external parameters (e.g., related to geometry, materials, temperature, etc.). Both numerator  $\mathbf{N}(s, \vartheta)$  and denominator  $\mathbf{D}(s, \vartheta)$  are constructed as a superposition of basis functions:  $\varphi_0(s) = 1$ ,  $\varphi_{n>0}(s) = (s - q_n)^{-1}$ , where  $q_n$  are fixed “basis poles”, are the standard partial fraction basis functions adopted in Vector Fitting (VF) schemes [2], and  $\xi_{\ell}(\vartheta)$  are multivariate (tensor-product) orthogonal (Chebychev) polynomials, here indexed by a unique global index  $\ell$  based on a suitable linear ordering.

The model coefficients  $\mathbf{R}_{n,\ell} \in \mathbb{R}^{P \times P}$  and  $r_{n,\ell} \in \mathbb{R}$  are computed by a *PSK iteration* [4], [8], [9], by minimizing the approximation error of the model with respect to input data samples  $\check{\mathbf{H}}_{k,m} = \check{\mathbf{H}}(j\omega_k, \vartheta_m)$ , the latter being available, e.g., from a parametric and frequency sweep of some full-wave solver. The following minimization problem

$$\min \left\| \frac{\mathbf{N}^{\mu}(j2\pi f_k, \vartheta_m) - \mathbf{D}^{\mu}(j2\pi f_k, \vartheta_m) \check{\mathbf{H}}_{k,m}}{\mathbf{D}^{\mu-1}(j2\pi f_k, \vartheta_m)} \right\| \quad (2)$$

is solved through successive iterations  $\mu = 1, 2, \dots$ , providing iterative coefficient estimates  $\mathbf{R}_{n,\ell}^{\mu}$  and  $r_{n,\ell}^{\mu}$ . Initialization is performed with  $\mathbf{D}^0 = 1$ , and the iteration is stopped when coefficient estimates stabilize.

The derivations in [4] show how to construct, starting from the model coefficients in (1), the following two (generalized) state-space realizations

$$\mathbf{H}(s; \vartheta) = \mathbf{C}(\vartheta)(s\mathbf{E} - \mathbf{A}(\vartheta))^{-1}\mathbf{B} \quad (3)$$

$$\mathbf{D}(s, \vartheta) = \mathbf{C}_D(\vartheta)(s\mathbf{I} - \mathbf{A}_D)^{-1}\mathbf{B}_D + D_D(\vartheta) \quad (4)$$

for the model  $\mathbf{H}(s; \vartheta)$  and its (scalar) denominator  $D(s, \vartheta)$ , respectively. Note that these realizations are parameter-dependent.

Assuming now the model to be in scattering representation, we define the following block-matrices

$$\begin{aligned}\mathbf{M}_\mathbf{H}(\vartheta) &= \begin{bmatrix} \mathbf{A}(\vartheta) & \mathbf{B}\mathbf{B}^\top \\ -\mathbf{C}^\top(\vartheta)\mathbf{C}(\vartheta) & -\mathbf{A}^\top(\vartheta) \end{bmatrix}, \quad \mathbf{K}_\mathbf{H} = \begin{bmatrix} \mathbf{E} & \mathbf{0} \\ \mathbf{0} & \mathbf{E}^\top \end{bmatrix} \\ \mathbf{M}_D(\vartheta) &= \begin{bmatrix} \mathbf{A}_D & \mathbf{0} & \mathbf{B}_D \\ \mathbf{0} & -\mathbf{A}_D^\top & -\mathbf{C}_D^\top(\vartheta) \\ \mathbf{C}_D(\vartheta) & \mathbf{B}_D^\top & 2D_D(\vartheta) \end{bmatrix}, \quad \mathbf{K}_D = \begin{bmatrix} \mathbf{I} & \mathbf{0} & \mathbf{0} \\ \mathbf{0} & \mathbf{I} & \mathbf{0} \\ \mathbf{0} & \mathbf{0} & \mathbf{0} \end{bmatrix}\end{aligned}$$

which are used to form the Skew-Hamiltonian/Hamiltonian (SHH) pencils  $(\mathbf{M}_\mathbf{H}(\vartheta), \mathbf{K}_\mathbf{H})$  and  $(\mathbf{M}_D(\vartheta), \mathbf{K}_D)$  for the complete model  $\mathbf{H}(s; \vartheta)$  and its denominator  $D(s, \vartheta)$ , respectively. Standard results in passivity theory [1] allow us to state that:

- If the denominator submodel  $D(s, \vartheta)$  is a Positive-Real function for any parameter value  $\vartheta$ , then the parameter-dependent poles  $p_n(\vartheta)$  are guaranteed stable  $\forall \vartheta$ . A sufficient condition for this uniform stability is that the SHH pencil  $(\mathbf{M}_D(\vartheta), \mathbf{K}_D)$  does not have any purely imaginary eigenvalues  $\forall \vartheta$ , together with the easily enforced asymptotic passivity condition  $D_D(\vartheta) > 0, \forall \vartheta$ .
- If the model is uniformly stable, a sufficient condition for the uniform passivity of the model  $\mathbf{H}(s; \vartheta)$  for all  $\vartheta$  is that the SHH pencil  $(\mathbf{M}_\mathbf{H}(\vartheta), \mathbf{K}_\mathbf{H})$  does not have any purely imaginary eigenvalues  $\forall \vartheta$  (again, with the asymptotic condition  $\|\mathbf{H}(\infty, \vartheta)\|_2 < 1 \forall \vartheta$ , which is easily enforced).

The above results lead to the conclusion that *both* stability and passivity of a multivariate model can be checked by computing Hamiltonian eigenvalues, and they are both enforced by making sure that no imaginary eigenvalues exist for any parameter value  $\vartheta \in \Theta$ . We deal with this latter requirement through an adaptive sampling technique, discussed below. We remark that, in case any imaginary eigenvalues are found, these can be removed by applying a standard perturbation scheme, suitably generalized to the multivariate case. Details are found in [7] for bivariate models (extension to the multivariate case is straightforward).

We now focus on our proposed adaptive sampling scheme in the parameter space  $\Theta$ , which has the purpose of detecting any region  $\Theta_q$  where at least one imaginary eigenvalue of the SHH pencil  $(\mathbf{M}(\vartheta), \mathbf{K})$  exists (we drop subscripts, since the adaptive search applies to both model and denominator pencils without differences). A first look at the numerical results depicted in the left panels of Fig. 1 helps us in establishing the goal: we would like to minimize the number of points  $\vartheta_i$  in the parameter space  $\Theta$  where the Hamiltonian pencil is constructed and its eigenvalues are computed, in order to detect all possible regions  $\Theta_q \subseteq \Theta$  where passivity is violated (depicted in red in the figure). The check must be conservative: we must not miss any small region  $\Theta_q$ , since this would imply loss of stability and/or passivity in the model.

We start by subdividing the entire parameter space  $\Theta$ , assumed to be a hypercube in  $\mathbb{R}^p$ , into smaller hypercubes based on a coarse uniform sampling. We use a binary subdivision of

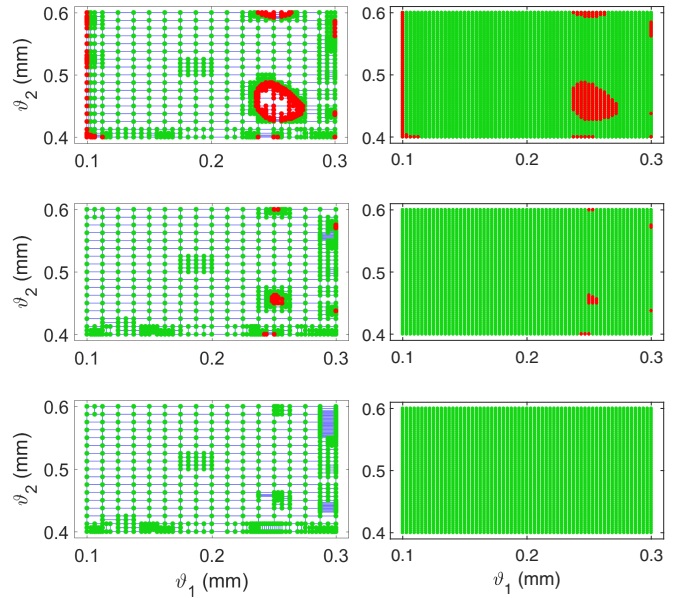


Fig. 1. Identification of regions  $\Theta_q \subseteq \Theta$  where at least one imaginary Hamiltonian eigenvalue exists (red dots: non-passive, green dots: passive). Left panels: results of proposed adaptive sampling scheme. Right panels: validation through a fine uniformly sampled grid. The three rows correspond to the passivity checks of three different iterations of a passivity enforcement scheme applied to a PCB interconnect macromodel.

each direction  $\nu$  into  $2^{j_0^\nu}$  segments. Normalizing the parameter space to the unit hypercube for simplicity, the result of this initialization is a set of disjoint segments if  $\rho = 1$ , rectangular patches if  $\rho = 2$  (the case depicted in Fig. 1), boxes if  $\rho = 3$ , and so on. In the following we only discuss the case  $\rho = 2$  with reference to Fig. 1. At all initial grid points, the eigenvalues of the Hamiltonian pencil are computed, and each point is flagged as “passive” or “non-passive” depending on the existence of imaginary eigenvalues.

After initialization, a hierarchical (binary) grid refinement loop is started. New evaluation points are added at the midpoint of each grid edge (the blue lines in Fig. 1), based on a local grid refinement criterion. This criterion is based on the following assumptions. For each considered edge:

- if both grid edge points are non-passive (there is at least one imaginary Hamiltonian eigenvalue of the pencil evaluated at both points), there is no need to refine: a region  $\Theta_q$  has already been found and both grid points are located inside this region;
- if one grid edge is passive and the other is not passive, the grid is always refined by adding a midpoint, in order to track the boundary of the passivity violation set  $\Theta_q$ ;
- if both grid edges are passive, a more advanced check is in order, since we must not miss a possible small-size region  $\Theta_q$  that might be located inbetween the two grid points. To this end, we perform a first-order perturbation analysis on *all* Hamiltonian eigenvalues (restricted to a single quadrant due to symmetry), as depicted in Fig. 2, in order to predict the location of these eigenvalues at one

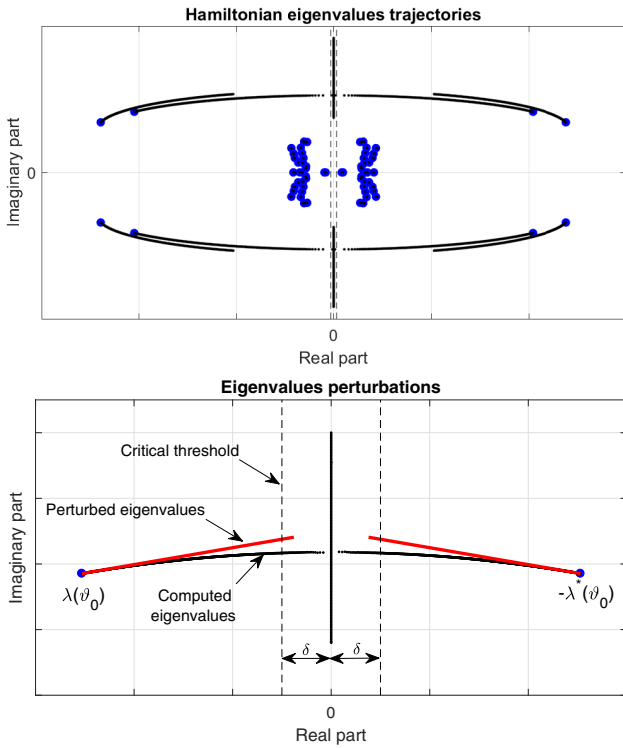


Fig. 2. Hamiltonian eigenvalues. Blue dots: eigenvalues  $\lambda_i(\vartheta_0)$  at a fixed parameter value  $\vartheta_0$ . Black lines: exact eigenvalue trajectories  $\lambda_i(\vartheta)$  for  $\vartheta = \vartheta_0 + \Delta\vartheta$ . Red lines: approximate eigenvalue trajectories  $\hat{\lambda}_i(\vartheta)$  based on linear perturbation theory.

grid edge through the perturbation of the eigenvalues at the other edge (and vice-versa). If any of these perturbations "move" the corresponding eigenvalue closer to the imaginary axis into a critical region (see the dashed lines in Fig. 2), then the grid is refined.

The above refinement checks are repeated for all elementary patches of the grid at current iteration. After all refinement points are added, the grid is post-processed by adding all required points that complete a multivariate binary subdivision into well-formed patches (boxes), and the refinement check is reiterated only on the new patches (boxes) that were formed at previous iteration. At the end of the refinement process, only a small subset of all possible grid points at the highest refinement level are checked (see Fig. 1).

The above-described adaptive sampling is performed without modifications for checking stability using the pencil  $(\mathbf{M}_D(\vartheta), \mathbf{K}_D)$ , and passivity using the pencil  $(\mathbf{M}_H(\vartheta), \mathbf{K}_H)$ . However, the results of the check are used in two different stages of model identification:

- the stability check is performed at each iteration of the PSK iteration (2). When the stability violation regions are localized, the corresponding stability conditions in terms of positivity of the denominator real part  $\text{Re}\left\{D(j\hat{\omega}_k, \hat{\vartheta}_m)\right\} > 0$  are formulated, where  $(\hat{\omega}_k, \hat{\vartheta}_m)$  are local minima of the denominator real part within each stability violation region  $\Theta_q$ . Such constraints are

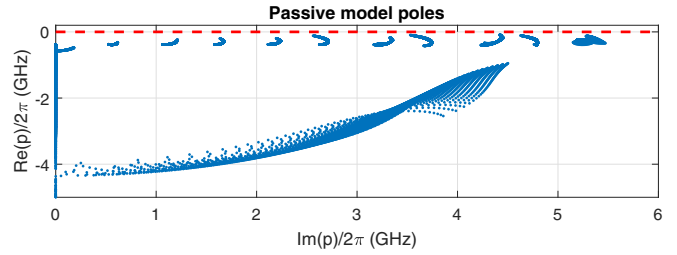


Fig. 3. Superposition of all poles computed for the PCB link parameterized model, instantiated at a finely sampled grid in the parameter space.

added to the PSK iteration, which becomes a linearly-constrained least squares problem, see more details in [8].

- the passivity check is performed within a passivity enforcement loop, which is run once an initial stable model is computed by the PSK iteration. In this stage, the model denominator is kept fixed, and the only variables that are optimized are the numerator coefficients. More details are available in [7].

Once a stable and passive multivariate model is available, a parameterized SPICE netlist can be synthesized [8], to be used for frequency- or time-domain what-if analyses and optimization using standard circuit solvers.

### III. NUMERICAL RESULTS

We illustrate our proposed passive macromodeling algorithm on a high-speed signal link (see [10]) running through two PCBs attached by a connector. The signal path is provided by a stripline (total PCB length 14 cm, permittivity  $\epsilon_r = 3$  with  $\tan\delta = 0.002$ ) connected by vertical vias located on the two sides of the connector and at the two input/output ports of the link. Each of these vias is surrounded by four ground vias (radius 127  $\mu\text{m}$  and distance from center via 762  $\mu\text{m}$ ). The structure is parameterized by the via radius  $\vartheta_1 \in [100, 300] \mu\text{m}$  and the corresponding antipad radius  $\vartheta_2 \in [400, 600] \mu\text{m}$ . The same structure was analyzed in [7], [8] by restricting the analysis to a single free parameter  $\vartheta_1$  or  $\vartheta_2$ . The electrical behavior of the structure is characterized through a set of sampled scattering responses (Courtesy of Prof. Christian Schuster and Dr. Jan Preibisch, Technische Universität Hamburg-Harburg, Hamburg, Germany), including  $\bar{k} = 250$  frequency samples up to 5 GHz for  $\bar{m} = 9 \times 9 = 81$  combinations of via radius and antipad radius values, linearly spaced within the design range.

The results of Fig. 1 illustrate the results of proposed passivity check at three different iterations of the model passivity enforcement loop, showing that all passivity violation regions are clearly identified by the proposed adaptive parameter sampling scheme. The last iteration (bottom panels) does not reveal any passivity violations, so we conclude that the model is uniformly passive throughout the parameter range.

Figure 4 compares the model responses (both return and insertion loss) to the corresponding raw data, by fixing one parameter ( $\vartheta_2$  in the left panels and  $\vartheta_1$  in the right panels),

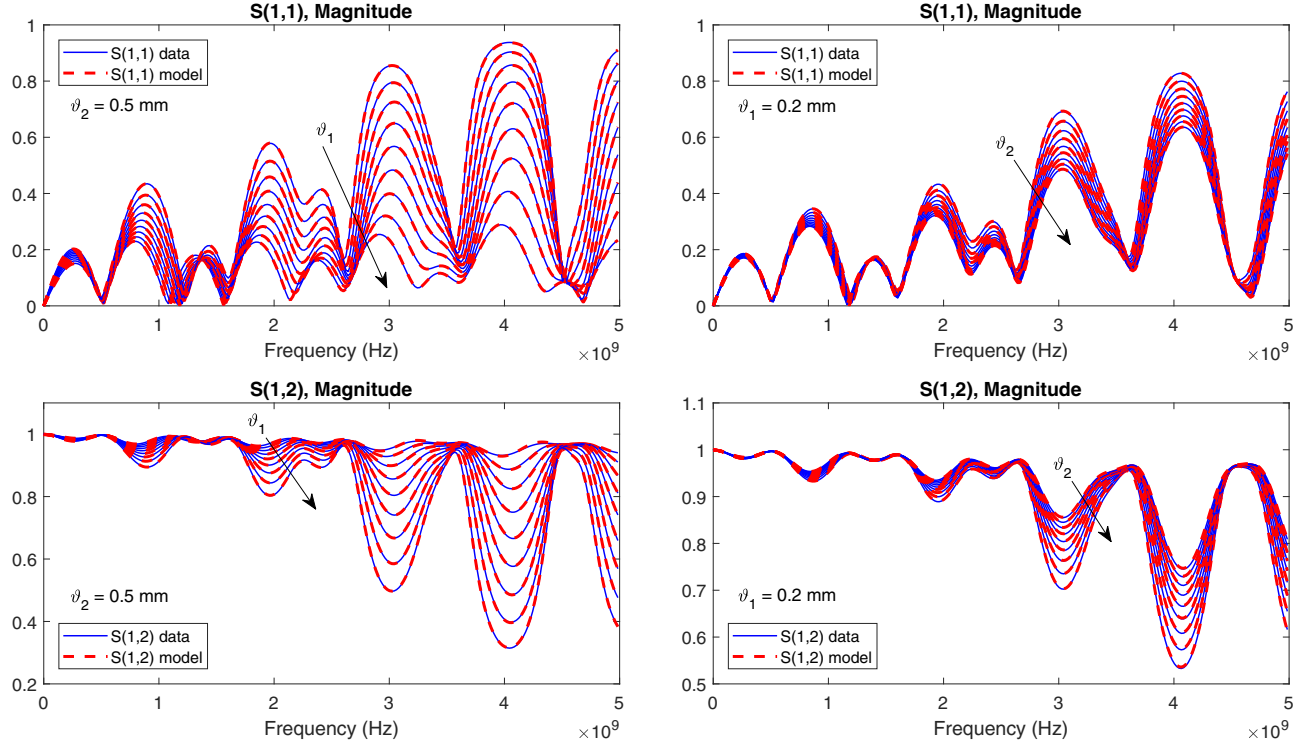


Fig. 4. Validation of a guaranteed stable and passive model of a PCB interconnect parameterized by via pad radius  $\vartheta_1$  and via antipad radius  $\vartheta_2$ .

and performing a sweep on the second. We observe that the model is accurate throughout the parameter space. Figure 3 depicts all the model poles of all model instances computed at all fine-grid (validation) points in the right panels of Fig. 1. This a-posteriori check confirms that the multivariate model is uniformly stable throughout the parameter space. The overall CPU time required to generate the models was 46 s, plus 12 min for passivity enforcement (total 5 iterations), using a standard laptop.

#### IV. CONCLUSIONS

We documented a systematic approach for the generation of stable and passive multivariate macromodels from sampled frequency responses. The models are identified using a constrained PSK iteration, which guarantees models with stable parameter-dependent poles. A post-processing step then enforces multivariate passivity. Both model stability and passivity constraints are based on the spectral characterization of a suitable Skew-Hamiltonian/Hamiltonian pencil. An adaptive sampling scheme in the parameter space is able to detect all stability/passivity violations, driving the formulation of stability and passivity constraints for iterative model construction. An illustrative two-parameter PCB interconnect example was used to illustrate the various steps of proposed algorithm.

As a final remark, we note that there cannot be a mathematical proof that the proposed adaptive scheme will not miss small residual passivity violations, since only a finite number of points are checked. However, this is extremely unlikely due to the rules that we use for grid refinement, combined

with the look-ahead properties of the Hamiltonian eigenvalue perturbation and with the smoothness of the singular value trajectories throughout the parameter/frequency space.

#### REFERENCES

- [1] S. Grivet-Talocia and B. Gustavsen, *Passive Macromodeling: Theory and Applications*. New York: John Wiley and Sons, 2016.
- [2] B. Gustavsen, A. Semlyen, “Rational approximation of frequency domain responses by vector fitting”, *IEEE Trans. Power Del.*, vol. 14, no. 3, pp. 1052–1061, July, 1999.
- [3] D. Deschrijver, M. Mrozowski, T. Dhaene, and D. De Zutter, “Macromodeling of multiport systems using a fast implementation of the vector fitting method,” *IEEE Microw. Wireless Comp. Lett.*, vol. 18, no. 6, pp. 383–385, Jun 2008.
- [4] P. Triverio, S. Grivet-Talocia, and M.S. Nakhla, “A Parameterized Macromodeling Strategy with Uniform Stability Test,” *IEEE Transactions on Advanced Packaging*, vol. 32, no. 1, pp. 205–215, Feb. 2009.
- [5] F. Ferranti, T. Dhaene, and L. Knockaert, “Compact and Passive Parametric Macromodeling Using Reference Macromodels and Positive Interpolation Operators,” *IEEE Trans. CPMT*, vol. 2, no. 12, pp. 2080–2088, Dec. 2012.
- [6] F. Ferranti, L. Knockaert, and T. Dhaene, “Passivity-Preserving Parametric Macromodeling by Means of Scaled and Shifted State-Space Systems,” *IEEE Trans. MTT*, vol. 59, no. 10, pp. 2394–2403, Oct. 2011.
- [7] S. Grivet-Talocia, “A Perturbation Scheme for Passivity Verification and Enforcement of Parameterized Macromodels”, *IEEE Trans. CPMT*, vol. 7, pp. 18691881, Nov 2017.
- [8] S. Grivet-Talocia, R. Trinchero, “Behavioral, Parameterized and Broadband Modeling of Wired Interconnects with Internal Discontinuities”, *IEEE Trans. EMC*, vol. 60, pp. 7785, Feb 2018
- [9] C. K. Sanathanan and J. Koerner, “Transfer function synthesis as a ratio of two complex polynomials,” *IEEE Trans. Automatic Control*, vol. 8, no. 1, pp. 56–58, Jan. 1963.
- [10] J. B. Preibisch, T. Reuschel, K. Scharff, J. Balachandran, B. Sen, C. Schuster, “Exploring Efficient Variability-Aware Analysis Method for High-Speed Digital Link Design Using PCE”, DesignCon, Jan 31-Feb 2, 2017, Santa Clara (CA), USA.